THE JOURNAL OF PHYSICAL CHEMISTRY C

Article

pubs.acs.org/JPCC

Gold Nanoparticles Modify the Photophysical and Photochemical Properties of 6-Thioguanine: Preventing DNA Oxidative Damage

Rennian Wang,[†,§] Ling Yue,[‡] Youqing Yu,[†] Xiaoran Zou,[†] Di Song,[†] Kunhui Liu,[‡] Yajun Liu,[‡] and Hongmei Su*[,†,‡,§]

[†]Beijing National Laboratory for Molecular Sciences (BNLMS), Institute of Chemistry, Chinese Academy of Sciences, Beijing 100190, China

[‡]College of Chemistry, Beijing Normal University, Beijing 100875, China

[§]University of Chinese Academy of Sciences, Beijing 100049, China

Supporting Information

ABSTRACT: For the widely used anticancer, antiinflammatory, and immunosuppressant drug 6-thioguanine (6-TG), its unique photochemistry of absorbing UVA, generating singlet oxygen ($^1O_2$), and inducing oxidative DNA damage can cause severe phototoxicity side effects in biomedical applications. Here we raise a new strategy of loading 6-TG onto gold nanoparticles (AuNPs) and demonstrate from systematic ultraviolet irradiation experiments that the 6-TG photochemistry can be successfully modulated by binding with AuNPs and the phototoxicity under UVA irradiation are effectively removed, not only for single base 6-TG but also for 6-TG embedded in DNA. In conjunction with excited state *ab initio* calculations, the molecular mechanisms are further unveiled, accounting for the protection effects of AuNPs in prohibiting the 6-TG photoactivation and $^1O_2$ oxidation. These findings point to tremendous possibilities of using AuNPs as inert carrier to modify excited state photochemistry and prevent unwanted phototoxicity effects of the adsorbed drug molecules.

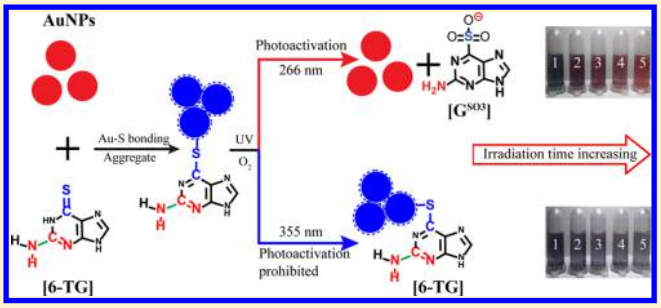

INTRODUCTION

As one of the most utilized anticancer, antiinflammatory, and immunosuppressant drugs, thiopurine has spurred strong research interests in medicinal, biological, and chemical fields since the discovery of its chemotherapeutic effects and the winning of the 1988 Noble Prize in Physiology or Medicine.[1] The thiopurines such as 6-thioguanine (6-TG), 6-mercaptopurine (6-MP), and azathioprine are all prodrugs (compounds that the body converts into active drugs) that are integrated into DNA as 6-TG by metabolism.[2−5] Most recent research has shown that thiopurine could even impair HIV replication.[6] However, patients who undergo long-term treatment of thiopurine drugs and sunshine exposure have a 50−200-fold increased incidence of skin cancer,[7,8] which is related to the unique photochemical and photophysical properties of 6-TG.[9−12] Unlike normal DNA bases that only absorb UVC and UVB light, 6-TG absorbs UVA light strongly and photosensitizes to generate singlet oxygen ($^1O_2$)[9−11] that invokes oxidative damage to cellular DNA and protein.[13−16] Meanwhile, 6-TG itself is vulnerable to the oxidation of $^1O_2$, resulting in the promutagenic product guanine-6-sulfonate (G^{SO3}) (Scheme 1).[9−12,17] G^{SO3} is unable to pair stably with normal DNA bases and then induces a rapid, profound, and irreversible block to DNA replication and transcription.[4,9,18−20]

Scheme 1. Illustration of the 6-TG Photochemistry upon UV Excitation

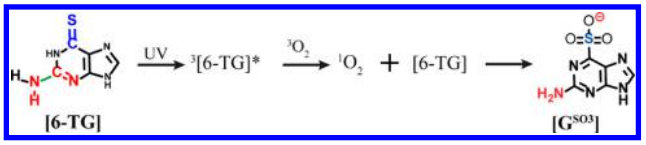

Such unusual photochemistry of 6-TG triggers events of DNA damage, causing harmful phototoxicity side effects *in vivo*. Several methods were tried to eliminate or prevent the unwanted deleterious effects of 6-TG, and one of the common strategies is using the antioxidants (e.g., ascorbate, *N*-acetylcysteine, β-mercaptoethanol, and cysteine) to alleviate the photochemical oxidation of 6-TG.[20,21] However, most antioxidants except ascorbate were found to react with the UVA-photoactivated 6-TG and 6-TG in oligodeoxynucleotides, forming other deleterious addition products via nucleophilic substitution.[21]

In this contribution, we report a new method to eliminate the 6-TG phototoxicity by loading 6-TG onto gold nanoparticles

Received: April 28, 2016
Revised: June 11, 2016
Published: June 13, 2016

DOI: 10.1021/acs.jpcc.6b04277
J. Phys. Chem. C 2016, 120, 14410−14415

(AuNPs). AuNPs are biocompatible and have unique physicochemical properties for transporting and unloading pharmaceuticals as drug carriers,[22−24] particularly for compounds bearing sulfur groups because of the strong binding affinity and Au−S bond formation.[25] It has been shown that the loading of 6-TG molecules onto AuNPs can enhance the intracellular drug uptake via the mechanism of endocytosis and improve the antiproliferation activity of 6-TG against cancer cells.[26] Furthermore, the unloading of 6-TG from AuNPs after internalization can be fulfilled in response to the intracellular stimulus glutathione (GSH).[27,28] These well-characterized studies[22−28] provide a basis for the practical use of AuNPs to deliver 6-TG drugs and prompt us to study the interaction of AuNPs with the photochemistry of 6-TG. Our study here based on a set of ultraviolet irradiation experiments and excited state *ab initio* calculations demonstrates for the first time that the photophysical and photochemical properties of 6-TG can be successfully modulated, after adsorbing onto the surface of AuNPs, through which the photoactivation of 6-TG to produce $^1O_2$ and the ensuing DNA damaging reactions are prohibited effectively.

EXPERIMENTAL AND THEORETICAL METHODS

Materials. 6-Thioguanine (Alfa Aesar), hydrogen tetrachloroaurate(III) trihydrate solution (Sigma-Aldrich), and sodium citrate dihydrate (Sigma-Aldrich) were used as received. The DNA oligonucleotides were purchased from the SBS Genetech Co., Ltd. (China) in the PAGE-purified form. To prepare the 6-TG dsDNA (5′-(6-TG)AAAAAAAGC-3′/5′-GCTTTTTTTC-3′), the same unit of ssDNA 5′-(6-TG)AAA-AAAAGC-3′ and the complementary strand 5′-GCTTT-TTTTC-3′ were dissolved in a buffer solution containing 10 mM Tris-HCl. The mixture was then heated to 90 °C for 5 min, slowly cooled to room temperature for 30 min, and stored in a refrigerator at 4 °C overnight. Ultrapure water (>18 MΩ·cm) obtained by Millipore filtration was used for all synthesis and solution preparations. All glassware and the magnetic stir bar were rigorously cleaned in freshly prepared aqua regia solution (HCl/HNO_3 = 3:1) and then rinsed by ultrapure water before use.

Synthesis of Gold Nanoparticles. Citrate-stabilized gold nanoparticles were prepared using published procedures.[29,30] Briefly, 143 mL of 2.8×10^{-4} M hydrogen tetrachloroaurate-(III) trihydrate solution was brought to boiling with refluxing; 7 mL of 38.8 mM sodium citrate tribasic dihydrate solution was added quickly under vigorous stirring. The solution was kept boiling and stirring for 15 min after the color changed to wine red. Then the solutions were cooled down to room temperature and filtered through a 0.22 μm nylon filter prior to use in order to avoid the undesirable nucleation. The prepared gold solution consists of dispersed spherical particles with a mean diameter of 15 ± 2 nm according to transmission electron microscopy (TEM) characterization. The concentration of the prepared gold solution was estimated to be 2.2 nM based on the size of nanoparticles, the amount of reactants, and the final volume of stock solution. TEM observations were carried out with a 300 keV Tecnai F30 transmission electron microscope. The TEM sample was prepared by dropping gold solution onto a copper grid.

Preparation of Sample Solutions and Irradiation Assay. 6-TG can induce the aggregation of AuNPs. With the addition of 6-TG, the color of AuNPs aqueous solution changed from wine red to purple. After incubation for 5 min the binding of 6-TG with AuNPs (1 nM) was completed, and the UV−vis absorption spectra for the mixed solution showed negligible change with time. Excess 6-TG were removed by centrifugation (14 000 rpm for 15 min), and the clear supernatant was taken off to remove the unbound 6-TG. The precipitate was redispersed in equal volume solution. This process was repeated for three times.[31] The final concentrations of 6-TG fully bound with AuNPs were determined by the UV−vis absorbance of 6-TG (2 μM).

For the 6-TG incorporated single-strand DNA (TG-ssDNA) and double-strand DNA (TG-dsDNA) binding with AuNPs, similar procedures were performed, except that the oligonucleotides solution was added into the AuNPs solution and incubated for 2 h at room temperature to ensure good binding according to previous study.[32] After removing the unbound oligonucleotides by centrifugation, the precipitate was redispersed in equal volume Tris-HCl (10 mM, pH 7.5). The DNA 6-TG concentrations fully bound with AuNPS were determined by monitoring the absorbance of 6-TG in the UV−vis spectra, which is 1.55 and 1. 37 μM for TG-ssDNA and TG-dsDNA, respectively.

The third harmonic (355 nm) and fourth harmonic (266 nm) of a Continuum Surelite II Nd:YAG laser beams were diverged and attenuated. Normally 2 mJ of energy was used to irradiate the sample solution in 1 cm quartz cuvettes. The UV−vis absorption and fluorescence spectra were measured to follow the photochemical reaction products. Samples were irradiated for a predetermined time and analyzed immediately after irradiation. The UV−vis absorption spectra were recorded with a UV−vis spectrometer (U-3010, Hitachi). Fluorescence emission spectra were measured using a Hitachi F-4600 fluorescence spectrophotometer.

Theoretical Calculation. Equilibrium geometries for the ground state (S_0), the lowest three excited singlet states (S_{1min}, S_{2min}, and S_{3min}), and the lowest two excited triplet states (T_{1min} and T_{2min}) were optimized by the SA-CASSCF method. The single point energies were calculated by SA-CASSCF and then refined by MS-CASPT2 calculations. The protocol is usually named MS-CASPT2//SA-CASSCF and has proved its accuracy repeatedly.[33,34] The vertical excitation energies and the relative energy profile for the geometric relaxation pathway were also calculated by this protocol. All the MS-CASPT2//SA-CASSCF calculations used an active space of 12 π electrons and 1 lone-pair electron distributed in 11 orbitals. Figure S3 shows the 11 orbitals used in the active space. In the state-averaged CASSCF calculations, equal state weights were used. In the MS-CASPT2 calculations, an imaginary level-shift correction of 0.2 au was applied to minimize the presence of intruder states.[35] All the calculations adopt the basis set of 6-31G(d) for C, N, O, and H atoms and 6-31+G(d,p) for the S atom. All geometry optimizations at the SA-CASSCF level were performed by using the MOLPRO 2010.1 package,[36] and the single point energy corrections at the MS-CASPT2 level were carried out by MOLCAS 7 package.[37]

RESULTS AND DISCUSSION

The photochemical reactions of 6-TG alone were investigated at first as a standard reference. According to the UV−vis absorption spectrum of 6-TG (Figure 1b), 266 and 355 nm lasers were selected to irradiate the O_2-saturated 6-TG aqueous solution, corresponding to the two absorption bands in the UVA and UVC region separately. Upon irradiation, photochemical reaction occurs, as manifested by the absorbance

DOI: 10.1021/acs.jpcc.6b04277
J. Phys. Chem. C 2016, 120, 14410−14415

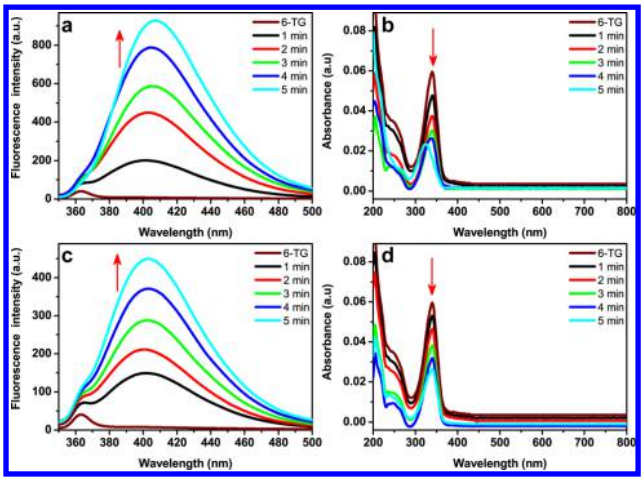

Figure 1. Fluorescence and UV−vis absorption spectra for the O_2-saturated 6-TG aqueous solution (2 μM) after (a, b) 266 nm irradiation and (c, d) 355 nm irradiation at various irradiation times. The excitation wavelength for fluorescence measurements was 320 nm. The ~360 nm peak in the fluorescence spectra is the Raman scattering band of the solvent water, which does not vary with the irradiation time. Arrows indicate the intensity change of the product fluorescence or 6-TG absorption peak with irradiation time.

decrease of 6-TG in the UV−vis absorption spectra (Figure 1b,d) and concomitant formation of the well-known fluorescent product G^{SO3} with emission at 408 nm in the fluorescence spectra (Figure 1a,c).[17,19,20] The formation of the cytotoxic G^{SO3} results from the successive oxidation of 6-TG by $^1O_2$ that is produced by triplet energy transfer after UV excitation of 6-TG (Scheme 1).[17,19,20] In the N_2-saturated solution under low O_2 conditions, the product yields of G^{SO3} were significantly reduced.

For 6-TG alone, irradiation at 266 or 355 nm can both trigger the $^1O_2$ formation and the oxidation of 6-TG by $^1O_2$ to G^{SO3}. To prevent 6-TG from photoactivation and oxidation, we used AuNPs as drug carrier in the following experiments. The citrate-stabilized AuNPs were synthesized by a conventional method.[29,30] The narrow plasmon resonance peak at 520 nm in the UV−vis absorption spectrum (Figure 2) and TEM image (inset i) indicate that the prepared AuNPs are monodispersed, with nearly the same diameter of ~15 ± 2 nm. Upon adding 6-TG, the loose citrate shell of the AuNPs could be replaced by 6-TG via exchange reaction,[38] forming the Au−S covalent bond and conjugating 6-TG with AuNPs. Without the stabilization of the negatively charged citrate, AuNPs aggregate (TEM in inset ii), and the color changed from wine red to purple instantly, with the 700 nm plasmon peak characteristic for the aggregated AuNPs[39] emerging in the UV−vis spectrum (Figure 2) as the monodispersed AuNPs peak at 520 nm was weakened.

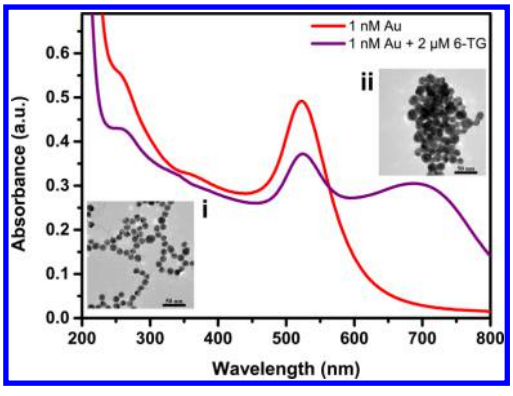

Figure 2. UV−vis absorption spectra for 1 nM AuNPs aqueous solution in the absence and the presence of 2 μM 6-TG. Inset: TEM image for AuNPs in the absence (i) and presence (ii) of 2 μM 6-TG (the scale bar represents 50 nm).

For probing surface chemistry of the adsorbed 6-TG onto AuNPs, centrifugation were taken to remove the excess 6-TG in bulk and solutions of 6-TG fully bound with AuNPs were prepared. The final concentration of 6-TG adsorbed on AuNPs (1 nM) is as low as 2 μM. Under such a low concentration, no signals for the phototoxicity-related transients (T_1 or $^1O_2$) in the transient spectra could be detected. Importantly, in the steady-state spectral measurements by probing end products G^{SO3}, the 6-TG photochemistry modified by AuNPs are allowed to be unveiled as follows.

When using 266 nm laser to irradiate the AuNPs/6-TG solution, the fluorescent product G^{SO3} with characteristic emission at 408 nm was still observed (Figure 3a), indicating the occurrence of the photooxidation, which is similar to the case of free 6-TG. The weaker fluorescence intensity of G^{SO3} here compared to Figure 1a should be due to AuNPs that can quench the fluorescence of adjacent molecules.[40,41] In addition, with the irradiation time increasing, the UV−vis spectra (Figure 3b) displayed an intensity decrease of the aggregation peak of AuNPs at 700 nm and concomitant increase of the 520 nm monodispersion peak; meanwhile, a series of color changes from purple to wine red (the inset in the Figure 3b) were observed. These results indicate that the 6-TG molecules are desorbed from AuNPs after being oxidized to G^{SO3}, leading to the disaggregation of the AuNPs. For G^{SO3}, because of the O−S bond formation, the Au−S bond is destroyed, and AuNPs get coated by citrate and become monodispersed again (Figure 3g).

Interestingly, for the UVA irradiation at 355 nm, it was observed that AuNPs can effectively prohibit the $^1O_2$ formation and the successive 6-TG oxidation by $^1O_2$. As shown in Figure 3c, no 408 nm emission characteristic to the oxidation product G^{SO3} was detected in the fluorescence spectra of the AuNPs/6-TG solution under prolonged 355 nm irradiation. Without undergoing photooxidation to produce G^{SO3}, 6-TG molecules still conjugate with AuNPs and AuNPs remain aggregated (Figure 3g), as evidenced by the negligible change of the AuNPs UV−vis absorption (Figure 3d) spectra and the unchanged purple color (inset) after irradiation. The unchanged UV−vis spectra and color of AuNPs/6-TG solution confirm further the absence of the G^{SO3} products at 355 nm. These results indicate that AuNPs protect 6-TG free from being oxidized to G^{SO3} under UVA (355 nm) irradiation and thus can prevent the DNA damage caused by G^{SO3} formation.

AuNPs absorb light broadly from the UV to visible region (Figure 2), with the plasmon peak at ~520 nm. Except exciting 6-TG, the 266 and 355 nm light may also excite AuNPs. Does the excitation of AuNPs affect the 6-TG photooxidation? Further control experiments of 532 nm irradiation (Figure 3e,f) were performed, where only AuNPs were excited. No fluorescent oxidation products G^{SO3} were detected, and thus no disaggregation of AuNPs was visible. Therefore, the excitation of AuNPs alone has no correlation with the photooxidation of 6-TG.

The photochemistry of 6-TG molecules adsorbed on AuNPs can be summarized in Figure 3g. Initially, conjugation of 6-TG with AuNPs by Au−S bond causes aggregation of AuNPs.

DOI: 10.1021/acs.jpcc.6b04277
J. Phys. Chem. C 2016, 120, 14410−14415

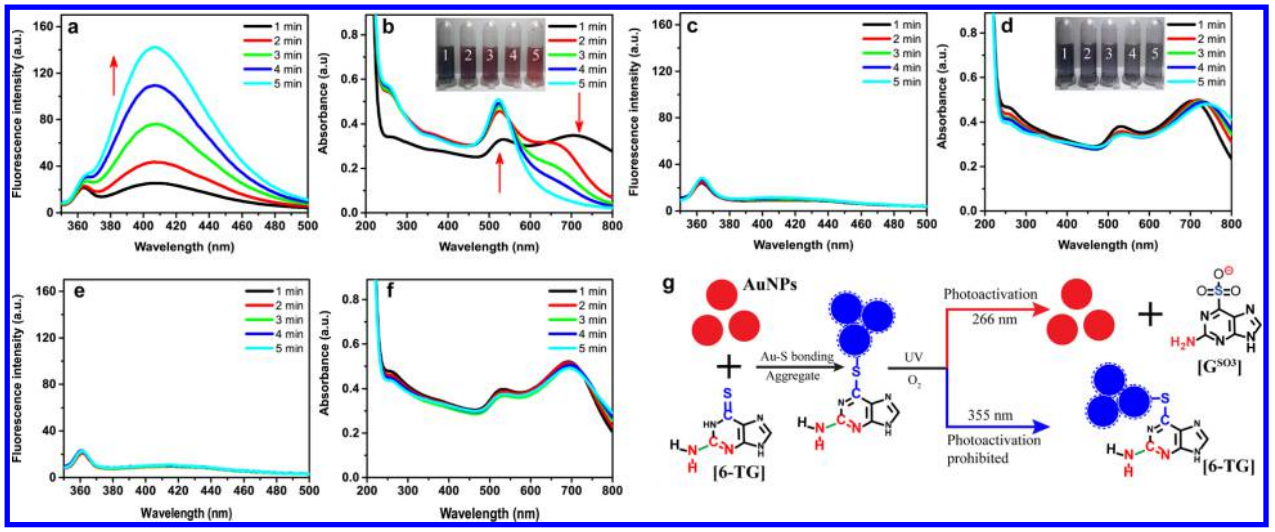

Figure 3. Fluorescence and UV−vis absorption spectra of O_2-saturated AuNPs (1 nM)/6-TG (2 μM) mixed solution upon irradiation of 266 nm (a, b), 355 nm (c, d), and 532 nm (e, f). The excitation wavelength for fluorescence measurements was 320 nm. Arrows indicate the intensity change of the product fluorescence or AuNPs plasmon peak with irradiation time. (g) Schematic illustration of the photochemistry of 6-TG adsorbed on AuNPs surface under UVC or UVA irradiation. Red and blue balls represent the monodispersed and aggregated AuNPs, respectively.

When 6-TG undergoes photooxidation to produce G^{SO3}, as in the case of 266 nm irradiation, the Au−S bond is destroyed and AuNPs return into the monodispersion state. On the other hand, when 6-TG photooxidation is prohibited by AuNPs, as in the case of 355 nm irradiation, no G^{SO3} is produced and AuNPs remain to be aggregated. For single base 6-TG, the sensitive color change of the irradiated AuNPs/6-TG solution makes AuNPs a colorimetric probe as well for such photochemical events.

After demonstrating the protection effect of AuNPs in preventing the photooxidation of single base 6-TG, we extended the studies to DNA 6-TG, i.e., the single-strand DNA (TG-ssDNA) and double-strand DNA (TG-dsDNA) with 6-TG incorporated. Unlike single base, TG-ssDNA or TG-dsDNA does not induce the aggregation of AuNPs, and the UV−vis absorption spectra exhibit only the 520 nm peak for monodispersed AuNPs (Figures S1 and S2). This is due to the extra negative charges that the phosphate groups (PO_4^{3-}) of DNA carry.[42] For the AuNPs/TG-ssDNA or AuNPs/TG-dsDNA mixed solution, irradiation experiments at 266, 355, and 532 nm were performed (Figures S1 and S2). In the fluorescence spectra, it shows that the photooxidation to produce G^{SO3} only occurs upon 266 nm irradiation and is totally suppressed under 355 nm irradiation, which is similar to the case of single base 6-TG. These experiments demonstrate further that in ssDNA and dsDNA with 6-TG incorporated AuNPs could effectively prevent 6-TG from photooxidation triggered by UVA (355 nm) excitation as well. This result is important for the realistic applications, since thiopurine drugs require to be incorporated into DNA as 6-TG by cell metabolism to take effect.[2−5] Here, it is demonstrated that the unique photochemistry of DNA 6-TG causing phototoxicity could be effectively prevented by the drug carrier AuNPs.

To understand the molecular mechanisms of AuNPs in affecting the photophysical and photochemical properties of 6-TG, we performed excited state *ab initio* calculations (see details in Supporting Information) which show that UVC (266 nm) and UVA (355 nm) populate the S_3 and S_2 states, respectively. The S_2 state is a $^1(\pi\pi^*)$ excitation corresponding to the transition from C═S/purine conjugated π orbital to π^* orbital (π_{CS} to π^*_{CS}, Figure 4 and Figure S3) with the elongation of the C═S bond (from 1.64 Å of S_0 to 2.02 Å of

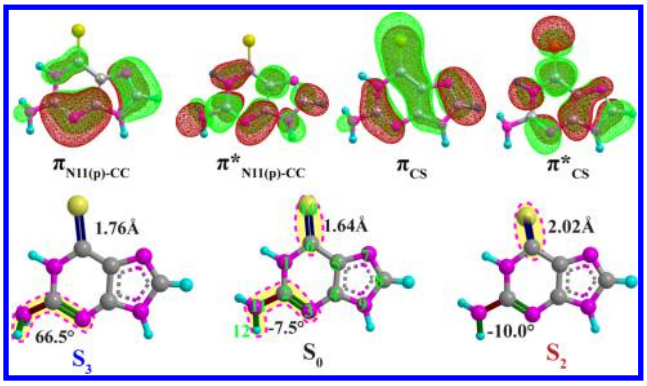

Figure 4. CASSCF optimized molecular orbitals related to the S_2 and S_3 excitation. Main structural parameters for the fully optimized geometries of S_0, S_2, and S_3 states calculated at MS-CASPT2//SA-CASSCF level (detailed structures displayed in Figure S4). Atomic numbering labeled in S_0. Yellow, gray, magenta, and cyan spheres represent sulfur, carbon, nitrogen, and hydrogen atoms, respectively.

S_2; see Figure 4). After excitation to S_2, a consecutive relaxation mechanism of S_2 to S_1, S_1 to T_2, and T_2 to T_1 through mutual energy crossings[43,44] allows for a drastically efficient intersystem crossing process (~0.3 ps)[45] to the lowest triplet state that ultimately leads to $^1O_2$ formation and the high phototoxicity of 6-TG. For the S_3 state, it is a $^1(\pi\pi^*)$ excitation from the p−π conjugated orbital between the N_{11} lone electron pair and the purine's aromatic π orbital to the aromatic π^* orbital ($\pi_{N11(p)\text{-}CC}$ to $\pi^*_{N11(p)\text{-}CC}$, Figure 4 and Figure S3), causing an obvious out-of-plane motion of the N_3−C_2−N_{11}−H_{12} dihedral angle (from −7.5° of S_0 to 66.5° of S_3; see Figure 4). S_3 interacts with other electronic states profoundly (Figure S5), resulting in favorable relaxation from S_3 to T_2 and T_2 to T_1 along with the $^1O_2$ phototoxicity under UVC excitation as well.

With the theoretical results, the modulation effects of AuNPs on 6-TG photochemistry can be understood. Under UVA (355 nm) light, the S_2 excitation corresponds to the transition from

DOI: 10.1021/acs.jpcc.6b04277
J. Phys. Chem. C 2016, 120, 14410−14415

C═S/purine conjugated π orbital to π^* orbital and is mainly correlated with the C═S bond deformation (Figure 4). After binding with AuNPs by forming the Au−S bond, the C═S double bond feature of 6-TG is removed and becomes a single bond within the infrastructure of C−S−Au (Figure 3g). In this case, the C═S/purine conjugated π orbital feature of 6-TG disappears. Therefore, the 355 nm light cannot excite 6-TG to the S_2 state anymore once these molecules are bound with AuNPs. Without being photoactivated, the photooxidation events of 6-TG are thus completely prohibited. On the other hand, the UVC (266 nm) light corresponds to S_3 excitation, which is mainly localized with the C_2-N_{11} bond, causing the $N_3-C_2-N_{11}-H_{12}$ dihedral angle change (Figure 4). In this case, Au−S bond formation between 6-TG and AuNPs has little effect on S_3 excitation. At 266 nm, 6-TG molecules can still be photoactivated to S_3 and undergo relaxation to T_1, leading to $^1O_2$ and oxidation. It turns out that the Au−S bond formation between 6-TG and AuNPs only modulates the S_2 excitation and thus prohibits the UVA photochemistry.

The effective elimination of the UVA phototoxicity of 6-TG by AuNPs observed here has important medicinal and biological implications. Unlike the canonical DNA bases that only absorb UVB and UVC, 6-TG is a UVA chromophore with a maximum absorption at 340 nm, causing UVA skin sensitivity and cancer risks for patients taking these drugs.[7,8] Meanwhile, UVA (320−400 nm) comprises more than 95% of the UV radiation in sunlight reaching earth organisms. Therefore, the detrimental phototoxicity of 6-TG is dominantly caused by UVA irradiation and the contribution from the shorter wavelength (~5%) UVB (320−290 nm) and UVC (290−200 nm) is minor. In view of this and given the well-characterized capability of AuNPs as drug carrier to deliver 6-TG, our observations here point to an effective measure of using AuNPs to remove these phototoxicity side effects of 6-TG *in vivo* for patients treated with thiopurine drugs.

CONCLUSION

In summary, we have shown that metal nanoparticles AuNPs can successfully modify the unique photochemistry of 6-TG that induces DNA oxidative damage. Conjugation of 6-TG with AuNPs by Au−S bond formation removes the double bond feature for the thiocarbonyl group of 6-TG, resulting in the prohibition of the UVA excitation to S_2 state for 6-TG since S_2 state corresponds mainly to the C═S bond excitation. Without undergoing photoactivation, the 6-TG photosensitization to form $^1O_2$ and the ensuing DNA oxidation events are effectively prevented, as evidenced by the absence of the major promutagenic product G^{SO3} in the fluorescence spectra for AuNPs/6-TG under UVA (355 nm) irradiation. Importantly, comparative experiments under UVC (266 nm) irradiation demonstrate this scenario from another aspect, where the photoactivation and oxidation of 6-TG to G^{SO3} still occur because the UVC light can excite 6-TG to S_3 state that is mainly related to the C_2-N_{11} bond excitation and barely affected by AuNPs conjugation. Altogether, these results provide new fundamental insights to understand the significant roles of AuNPs in affecting the excited state photochemistry of the adsorbed molecules.

Of paramount importance for the application of AuNPs as drug carrier, we have demonstrated that AuNPs can remove efficiently the UVA phototoxicity side effects of 6-TG that is the main cause for the increased incidence of skin cancers in patients under thiopurine treatment. In fact, 6-TG represents an important class of drugs based on thiobases (4-thiothymidine, 2-thiothymidine, 4-thiouracil, 2-thiouracil, 6-mercaptopurine, etc.) that have the photochemical properties of generating $^1O_2$ by UVA absorption and photosensitization.[46−49] Therefore, the pronounced protection effects of AuNPs in preventing the harmful phototoxicity of 6-TG and improve the drug efficacy can be extended to a class of thiobase drugs in principle, and further related studies should be of high interest.

ASSOCIATED CONTENT

Supporting Information

The Supporting Information is available free of charge on the ACS Publications website at DOI: 10.1021/acs.jpcc.6b04277.

Additional experimental and calculation results (PDF)

AUTHOR INFORMATION

Corresponding Author

*E-mail hongmei@iccas.ac.cn or hongmei@bnu.edu.cn; Tel 86-10-62562837 (H.S.).

Notes

The authors declare no competing financial interest.

ACKNOWLEDGMENTS

This work was financially supported by the National Natural Science Foundation of China (Grant No. 21333012, 21425313) and the National Basic Research Program of China (2013CB834602).

REFERENCES

(1) Elion, G. B. The Purine Path to Chemotherapy. *Science* **1989**, *244*, 41−47.
(2) Lennard, L.; Lilleyman, J. S.; Van Loon, J.; Weinshilboum, R. M. Genetic Variation in Response to 6-Mercaptopurine for Childhood Acute Lymphoblastic Leukaemia. *Lancet* **1990**, *336*, 225−229.
(3) Waters, T. R.; Swann, P. F. Cytotoxic Mechanism of 6-Thioguanine: hMutSα, the Human Mismatch Binding Heterodimer, Binds to DNA Containing S6-Methylthioguanine. *Biochemistry* **1997**, *36*, 2501−2506.
(4) Brem, R.; Karran, P. Multiple Forms of DNA Damage Caused by UVA Photoactivation of DNA 6-Thioguanine. *Photochem. Photobiol.* **2012**, *88*, 5−13.
(5) Weinshilboum, R. Thiopurine Pharmacogenetics: Clinical and Molecular Studies of Thiopurine Methyltransferase. *Drug Metab. Dispos.* **2001**, *29*, 601−605.
(6) Narukawa, M.; Shimizu, S.; Hacke, K.; Treger, J.; Cortado, R.; Egger, E.; Kasahara, N.; An, D. S. Efficient Selection of Genetically Engineered HIV Resistant Cells by Short Hairpin RNA Mediated HPRT and CCR5 Knockdown. *Mol. Ther.* **2013**, *21*, S204−S205.
(7) Ramsay, H. M.; Fryer, A. A.; Hawley, C. M.; Smith, A. G.; Nicol, D. L.; Harden, P. N. Non-Melanoma Skin Cancer Risk in the Queensland Renal Transplant Population. *Br. J. Dermatol.* **2002**, *147*, 950−956.
(8) Euvrard, S.; Kanitakis, J.; Claudy, A. Skin Cancers after Organ Transplantation. *N. Engl. J. Med.* **2003**, *348*, 1681−1691.
(9) O'Donovan, P.; Perrett, C. M.; Zhang, X. H.; Montaner, B.; Xu, Y. Z.; Harwood, C. A.; McGregor, J. M.; Walker, S. L.; Hanaoka, F.; Karran, P. Azathioprine and UVA Light Generate Mutagenic Oxidative DNA Damage. *Science* **2005**, *309*, 1871−1874.
(10) Brem, R.; Li, F.; Karran, P. Reactive Oxygen Species Generated by Thiopurine/UVA Cause Irreparable Transcription-Blocking DNA Lesions. *Nucleic Acids Res.* **2009**, *37*, 1951−1961.
(11) Zhang, Y.; Zhu, X.; Smith, J.; Haygood, M. T.; Gao, R. Direct Observation and Quantitative Characterization of Singlet Oxygen in

Aqueous Solution Upon UVA Excitation of 6-Thioguanines. *J. Phys. Chem. B* **2011**, *115*, 1889−1894.
(12) Brem, R.; Daehn, I.; Karran, P. Efficient DNA Interstrand Crosslinking by 6-Thioguanine and UVA Radiation. *DNA Repair* **2011**, *10*, 869−876.
(13) Favre, A.; Saintome, C.; Fourrey, J. L.; Clivio, P.; Laugaa, P. Thionucleobases as Intrinsic Photoaffinity Probes of Nucleic Acid Structure and Nucleic Acid Protein Interactions. *J. Photochem. Photobiol., B* **1998**, *42*, 109−124.
(14) Cadet, J.; Doukid, T.; Ravanatd, J.-L.; Di Masciof, P. In *Singlet Oxygen: Applications in Biosciences and Nanosciences*; Nonell, S., Flors, C., Eds.; Royal Society of Chemistry: 2016; Vol. *1*, pp 393−407.
(15) Ravanat, J.-L.; Di Mascio, P.; Martinez, G. R.; Medeiros, M. H.; Cadet, J. Singlet Oxygen Induces Oxidation of Cellular DNA. *J. Biol. Chem.* **2000**, *275*, 40601−40604.
(16) Cadet, J.; Douki, T.; Pouget, J. P.; Ravanat, J. L. Singlet Oxygen DNA Damage Products: Formation and Measurement. *Methods Enzymol.* **2000**, *319*, 143−153.
(17) Zou, X.; Zhao, H.; Yu, Y.; Su, H. Formation of Guanine-6-Sulfonate from 6-Thioguanine and Singlet Oxygen: A Combined Theoretical and Experimental Study. *J. Am. Chem. Soc.* **2013**, *135*, 4509−4515.
(18) Brem, R.; Karran, P. Oxidation-Mediated DNA Cross-Linking Contributes to the Toxicity of 6-Thioguanine in Human Cells. *Cancer Res.* **2012**, *72*, 4787−4795.
(19) Zhang, X. H.; Jeffs, G.; Ren, X. L.; O'Donovan, P.; Montaner, B.; Perrett, C. M.; Karran, P.; Xu, Y. Z. Novel DNA Lesions Generated by the Interaction between Therapeutic Thiopurines and UVA Light. *DNA Repair* **2007**, *6*, 344−354.
(20) Ren, X. L.; Li, F.; Jeffs, G.; Zhang, X.; Xu, Y. Z.; Karran, P. Guanine Sulphinate Is a Major Stable Product of Photochemical Oxidation of DNA 6-Thioguanine by UVA Irradiation. *Nucleic Acids Res.* **2010**, *38*, 1832−1840.
(21) Ren, X. L.; Xu, Y. Z.; Karran, P. Photo-Oxidation of 6-Thioguanine by UVA: The Formation of Addition Products with Low Molecular Weight Thiol Compounds. *Photochem. Photobiol.* **2010**, *86*, 1038−1045.
(22) Ghosh, P.; Han, G.; De, M.; Kim, C. K.; Rotello, V. M. Gold Nanoparticles in Delivery Applications. *Adv. Drug Delivery Rev.* **2008**, *60*, 1307−1315.
(23) Sun, T.; Zhang, Y. S.; Pang, B.; Hyun, D. C.; Yang, M.; Xia, Y. Engineered Nanoparticles for Drug Delivery in Cancer Therapy. *Angew. Chem., Int. Ed.* **2014**, *53*, 12320−12364.
(24) Huo, S.; Jin, S.; Ma, X.; Xue, X.; Yang, K.; Kumar, A.; Wang, P. C.; Zhang, J.; Hu, Z.; Liang, X.-J. Ultrasmall Gold Nanoparticles as Carriers for Nucleus-Based Gene Therapy Due to Size-Dependent Nuclear Entry. *ACS Nano* **2014**, *8*, 5852−5862.
(25) Grönbeck, H.; Curioni, A.; Andreoni, W. Thiols and Disulfides on the Au(111) Surface: The Headgroup-Gold Interaction. *J. Am. Chem. Soc.* **2000**, *122*, 3839−3842.
(26) Podsiadlo, P.; Sinani, V. A.; Bahng, J. H.; Kam, N. W. S.; Lee, J.; Kotov, N. A. Gold Nanoparticles Enhance the Anti-Leukemia Action of a 6-Mercaptopurine Chemotherapeutic Agent. *Langmuir* **2008**, *24*, 568−574.
(27) Ock, K.; Jeon, W. I.; Ganbold, E. O.; Kim, M.; Park, J.; Seo, J. H.; Cho, K.; Joo, S.-W.; Lee, S. Y. Real-Time Monitoring of Glutathione-Triggered Thiopurine Anticancer Drug Release in Live Cells Investigated by Surface-Enhanced Raman Scattering. *Anal. Chem.* **2012**, *84*, 2172−2178.
(28) Hong, R.; Han, G.; Fernández, J. M.; Kim, B.-j.; Forbes, N. S.; Rotello, V. M. Glutathione-Mediated Delivery and Release Using Monolayer Protected Nanoparticle Carriers. *J. Am. Chem. Soc.* **2006**, *128*, 1078−1079.
(29) Turkevich, J.; Stevenson, P. C.; Hillier, J. A Study of the Nucleation and Growth Processes in the Synthesis of Colloidal Gold. *Discuss. Faraday Soc.* **1951**, *11*, 55−75.
(30) Frens, G. Controlled Nucleation for the Regulation of the Particle Size in Monodisperse Gold Suspensions. *Nature, Phys. Sci.* **1973**, *241*, 20−22.
(31) Ansar, S. M.; Perera, G. S.; Ameer, F. S.; Zou, S.; Pittman, C. U.; Zhang, D. Desulfurization of Mercaptobenzimidazole and Thioguanine on Gold Nanoparticles Using Sodium Borohydride in Water at Room Temperature. *J. Phys. Chem. C* **2013**, *117*, 13722−13729.
(32) Seela, F.; Ding, P.; Budow, S. DNA Gold Nanoparticle Conjugates Incorporating Thiooxonucleosides: 7-Deaza-6-Thio-2′-Deoxyguanosine as Gold Surface Anchor. *Bioconjugate Chem.* **2011**, *22*, 794−807.
(33) Andersson, K.; Malmqvist, P. Å.; Roos, B. O. Second-Order Perturbation Theory with a Complete Active Space Self-Consistent Field Reference Function. *J. Chem. Phys.* **1992**, *96*, 1218−1226.
(34) Roos, B. O.; Andersson, K.; Fülscher, M. P.; Malmqvist, P.-â.; Serrano-Andrés, L.; Pierloot, K.; Merchán, M. In *New Methods in Computational Quantum Mechanics*; Prigogine, I., Rice, S. A., Eds.; John Wiley & Sons, Inc.: Hoboken, NJ, 2007; Vol. *93*, pp 219−331.
(35) Forsberg, N.; Malmqvist, P.-Å. Multiconfiguration Perturbation Theory with Imaginary Level Shift. *Chem. Phys. Lett.* **1997**, *274*, 196−204.
(36) Werner, H.-J.; Knowles, P. J.; Knizia, G.; Manby, F. R.; Schütz, M. Molpro: A General-Purpose Quantum Chemistry Program Package. *Wiley Interdiscip. Rev. Comput. Mol. Sci.* **2012**, *2*, 242−253.
(37) Karlström, G.; Lindh, R.; Malmqvist, P.-Å.; Roos, B. O.; Ryde, U.; Veryazov, V.; Widmark, P.-O.; Cossi, M.; Schimmelpfennig, B.; Neogrady, P.; Seijo, L. MOLCAS: A Program Package for Computational Chemistry. *Comput. Mater. Sci.* **2003**, *28*, 222−239.
(38) Fendler, J. H. Chemical Self-Assembly for Electronic Applications. *Chem. Mater.* **2001**, *13*, 3196−3210.
(39) Norman, T. J.; Grant, C. D.; Magana, D.; Zhang, J. Z.; Liu, J.; Cao, D.; Bridges, F.; Van Buuren, A. Near Infrared Optical Absorption of Gold Nanoparticle Aggregates. *J. Phys. Chem. B* **2002**, *106*, 7005−7012.
(40) Chhabra, R.; Sharma, J.; Wang, H.; Zou, S.; Lin, S.; Yan, H.; Lindsay, S.; Liu, Y. Distance-Dependent Interactions between Gold Nanoparticles and Fluorescent Molecules with DNA as Tunable Spacers. *Nanotechnology* **2009**, *20*, 485201.
(41) Samanta, A.; Zhou, Y.; Zou, S.; Yan, H.; Liu, Y. Fluorescence Quenching of Quantum Dots by Gold Nanoparticles: A Potential Long Range Spectroscopic Ruler. *Nano Lett.* **2014**, *14*, 5052−5057.
(42) Sharma, J.; Chhabra, R.; Liu, Y.; Ke, Y.; Yan, H. DNA-Templated Self-Assembly of Two-Dimensional and Periodical Gold Nanoparticle Arrays. *Angew. Chem., Int. Ed.* **2006**, *45*, 730−735.
(43) Martínez-Fernández, L.; González, L.; Corral, I. An ab initio Mechanism for Efficient Population of Triplet States in Cytotoxic Sulfur Substituted DNA Bases: The Case of 6-Thioguanine. *Chem. Commun.* **2012**, *48*, 2134−2136.
(44) Martínez-Fernández, L.; Corral, I.; Granucci, G.; Persico, M. Competing Ultrafast Intersystem Crossing and Internal Conversion: A Time Resolved Picture for the Deactivation of 6-Thioguanine. *Chem. Sci.* **2014**, *5*, 1336−1347.
(45) Reichardt, C.; Guo, C.; Crespo-Hernández, C. E. Excited-State Dynamics in 6-Thioguanosine from the Femtosecond to Microsecond Time Scale. *J. Phys. Chem. B* **2011**, *115*, 3263−3270.
(46) Pollum, M.; Martínez-Fernández, L.; Crespo-Hernández, C. In *Photoinduced Phenomena in Nucleic Acids I*; Barbatti, M., Borin, A. C., Ullrich, S., Eds.; Springer International Publishing: 2015; Vol. *355*, pp 245−327.
(47) Pollum, M.; Crespo-Hernández, C. E. Communication: The Dark Singlet State as a Doorway State in the Ultrafast and Efficient Intersystem Crossing Dynamics in 2-Thiothymine and 2-Thiouracil. *J. Chem. Phys.* **2014**, *140*, 071101.
(48) Pollum, M.; Jockusch, S.; Crespo-Hernández, C. E. 2,4-Dithiothymine as a Potent UVA Chemotherapeutic Agent. *J. Am. Chem. Soc.* **2014**, *136*, 17930−17933.
(49) Pollum, M.; Jockusch, S.; Crespo-Hernández, C. E. Increase in the Photoreactivity of Uracil Derivatives by Doubling Thionation. *Phys. Chem. Chem. Phys.* **2015**, *17*, 27851−27861.

DOI: 10.1021/acs.jpcc.6b04277
J. Phys. Chem. C 2016, 120, 14410−14415